

Polypropylene-based nano-composite formation: Delamination of organically modified layered filler via solid-state processing

Tomotaka Saito ^a, Masami Okamoto ^{b,*}

^a Research Laboratories, Toyota Boshoku Co. Ltd., 1-1, Toyoda-Chō, Kariya 448-8651, Japan

^b Advanced Polymeric Nanostructured Materials Engineering, Graduate School of Engineering, Toyota Technological Institute, Hisakata 2-12-1, Tempaku, Nagoya 468-8511, Japan

ARTICLE INFO

Article history:

Received 20 April 2010

Received in revised form

15 June 2010

Accepted 25 June 2010

Keywords:

Delamination

Solid-state processing

Layered fillers

ABSTRACT

Solid-state processing for the preparation of polypropylene (PP)-based nano-composites having finely dispersed layered fillers was conducted. The mixture of PP and organically modified layered filler (OMLF) (95:5 wt./wt.) was subjected to the processing using alumina mortar heated 65 °C, below T_m of PP (i.e., PP is still at the solid-state), and ground for 8 h before melt compounding. On X-ray diffraction, the $d_{(001)}$ peak of OMLF was broaden and peak position shifted slightly. The mixture prepared by solid-state processing exhibited disorder and delaminated layer structure with the thickness of 3–7 nm into PP matrix through TEM observations. On the contrary, nano-composite prepared by melt compounding at 180 °C for 3 min (without solid-state processing) showed the large stacked silicate layers in the PP matrix. Furthermore, instead of using alumina mortar, we carried out solid-state processing using internal mixer. X-ray diffraction pattern and TEM observation exhibited similar results. The solid-state processing led to delamination of the silicate layers and attained the discrete dispersion.

© 2010 Elsevier Ltd. All rights reserved.

1. Introduction

A significant amount of work has already done on various aspects of polymeric nano-composite containing organically modified layered fillers (OMLFs) [1]. However, complete delamination of OMLFs in continuous polymer matrix is still challenging issue because it could not be satisfactorily attained. Gardolinski and Lagaly [2] described a very distinctive definition of delamination and exfoliation in aim to avoid the controversial use of these terms. Exfoliation is defined as the decomposition of large aggregates into smaller particles, whereas delamination denotes the process of separation of the individual layers of the particles at the nanoscale.

To the best of our knowledge, so far, the complete delamination is not feasible after melt intercalation with appropriate shear. Only a few examples of this type can be found in the literature [3,4], but many published photographs show very small regions in the melt compound where partially exfoliation occurred [1]. Delamination of stacked layered fillers in polymeric nano-composite is the ultimate target for controlling better overall materials' properties. Thus, we are far from the goal of understanding the mechanisms of the nano-structure control and the preparation of the

nano-composite with discrete dispersion of the nano-fillers. From this reason, a novel preparation method is currently in progress.

Some methods for the delamination of OMLFs were conducted by using supercritical CO₂ [5,6]. The effect of the supercritical CO₂ (sc-CO₂) fed to the tandem extruder on the dispersion of organically modified montmorillonite (MMT) with different intercalants into Nylon 6 matrix was examined [6]. In the absence of sc-CO₂, pressure improved the MMT-clay delamination by reducing the free volume of the polymer and increasing the interaction between chains and ultimately increasing the viscosity. Using sc-CO₂ did not improve the clay dispersion due to the decreasing the melt viscosity. Another interesting approach for the delamination of OMLFs is an ultrasound in the preparation of nano-composites. The effect of the *in-situ* ultrasound on the polymer/MMT melt phase is reported [7].

An effective method to enhance the dispersion, intercalation and exfoliation of OMLFs in thermoplastic-based nano-composites is reported. The same experiment was done in another report for polypropylene (PP)-base nano-composite preparation [8]. The maximum power output and frequency of the ultrasonic generator are 300W and 20 kHz, respectively. They described the fine dispersion of silicate layers in PP matrix after ultrasonic treatment (100W). However, the ultrasonic oscillations exhibited a little effect on the delamination of OMLFs as revealed by transmission electron microscope (TEM) observation. Thus, the compounding with an assist from sc-CO₂ fluids and ultra-sonication did not improve the

* Corresponding author. Fax: +81 (0) 52 809 1864.

E-mail address: okamoto@toyota-ti.ac.jp (M. Okamoto).

state of the nano-filler dispersion once a critical morphology was established. That is, the dispersion of the nano-filler in the polymer matrix is governed by judicious choice of OMLF.

Although the intercalation technology of the polymer melt is developed along with the current industrial process, such as extrusion and injection molding, we have to develop more innovative compounding process, especially in the preparation of the nano-composites possessing discrete dispersion of the nano-fillers.

In this regard, we have reported solid-state processing of poly(*p*-phenylenesulfide) (PPS)-based nano-composites to delaminate the stacked, layered filler in the polymer matrix [9,10]. The mixture of PPS and organically modified layered filler (OMLF) (95:5 wt./wt.) was subjected to the processing using thermostatted hot-press at ambient temperature and 150 °C, below T_m of PPS (i.e., PPS matrix is still at the solid-state), and applying pressures of 7, 14 and 33 MPa for 30s. The mixture exhibited disorder and delaminated layer structure with the thickness of 40–80 nm into PPS matrix. The solid-state processing led to delamination of the silicate layers and attained the discrete dispersion. Similarly, Wang et al. [11–13] reported the exfoliation of talc fillers by solid-state shear processing using pan-type mill, to prepare PP/talc nano-composites, in which the delamination of talc fillers was not achieved in the nano-composite as revealed by TEM images.

Wakabayashi et al. [14] demonstrated that a continuous scalable solid-state shear pulverization (SSSP) could result in well-dispersed unmodified graphite in PP, leading to a 100% increase in modulus as compared with neat PP. High shear and compressive forces result in repeated fragmentation and fusion of polymer in the solid-state producing excellent mixing and dispersion of nano-fillers in the nano-composites [15].

The solid-state shear processing may be an innovative technique to delaminate the layered fillers in overcoming the pressure drop (Δp) within the nano-galleries [10]. Therefore, successful delamination of OMLFs could broaden the scope of application of this procedure. The objective of this work is to gain insight into the solid-state processing for the preparation of nano-composites based on PP having finely dispersed layered fillers.

2. Experimental

Organically modified layered filler (OMLF) used in this study was montmorillonite (MMT, Hojun Co., Ltd.) intercalated with *n*-hexadecyl tri-*n*-butyl phosphonium (C_{16} TBP) cation. A polypropylene (PP) fine powder (average particle size ~5 μm, T_m = 151 °C), purchased from Seishin enterprise Co., Ltd. The homogeneous mixture of PP and OMLF in the weight ratio 95/5 was prepared. We have ground the mixture with pestle and mortar for 8 h at 65 °C (well below T_m of PP matrix powder). We call the process “solid-state processing” because PP matrix is solid-state. After solid-state processing, the mixture of PP and OMLF was melt compounded using miniature mixer of gram scale (MINI-MAX Molder CS-183, Custom Scientific Instruments Inc.) and to convert into sheet for the characterization.

The nano-structure analyses of wide-angle X-ray diffraction (WAXD) were performed for the PP/OMLF mixture and corresponding nano-composite sheets by using MXlabo X-ray diffractometer (MAC Science Co., CuK α radiation, wavelength λ = 0.154 nm) and Ultima IV X-ray diffractometer (Rigaku Co., CuK α radiation, wavelength λ = 0.154 nm), and transmission electron microscopy (TEM) were carried out using the same apparatus as in the previous articles [9]. To investigate the micro-scale morphology of the nano-composites, we also used polarizing optical microscope (POM). The detail of POM observation is in our previous paper [10]. For analyzing the features of the micrographs, we carried out fast Fourier transform (FFT) analysis on digitally saved images of POM

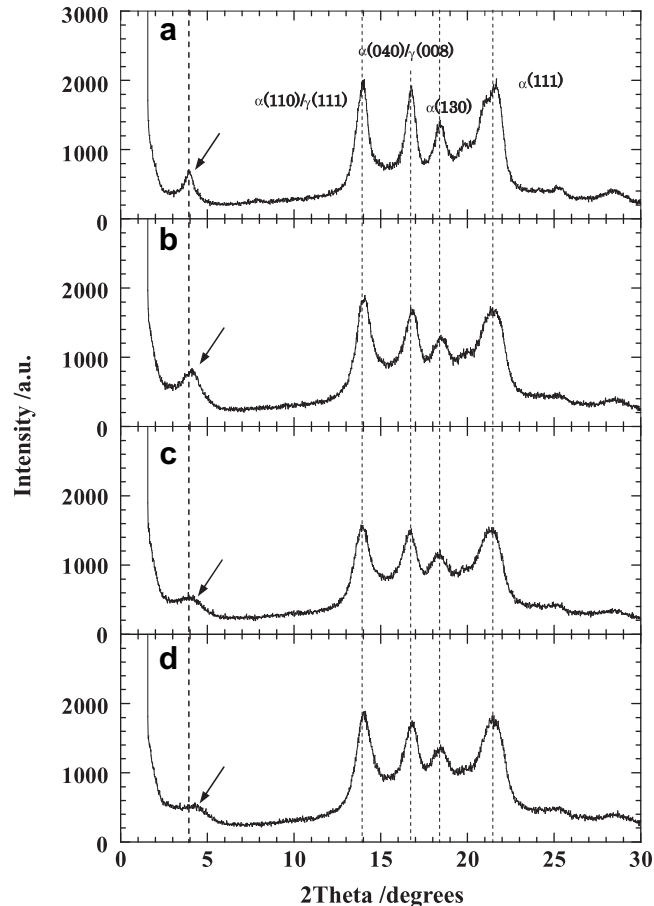


Fig. 1. WAXD patterns of (a) mixture of PP and OMLF (95:5 wt./wt.) before solid-state processing, (b), (c) and (d) processed mixture of PP/OMLF at 65 °C for 1, 2 and 8 h, respectively. Arrows in each panel indicate $d_{(001)}$ peak of OMLF. The strong diffraction peaks at $2\theta = 15\text{--}25^\circ$ are assigned to the monoclinic (α -form)/triclinic (γ -form) unit cells of the crystallized PP.

and TEM micrographs using the commercial image analysis software (Ultimage®, Graftek, France) [16], which allowed to provide us information equivalent to the scattering analyses.

For comparison, the PP-based nano-composite preparation was conducted via conventional melt compounding operated at 180 °C

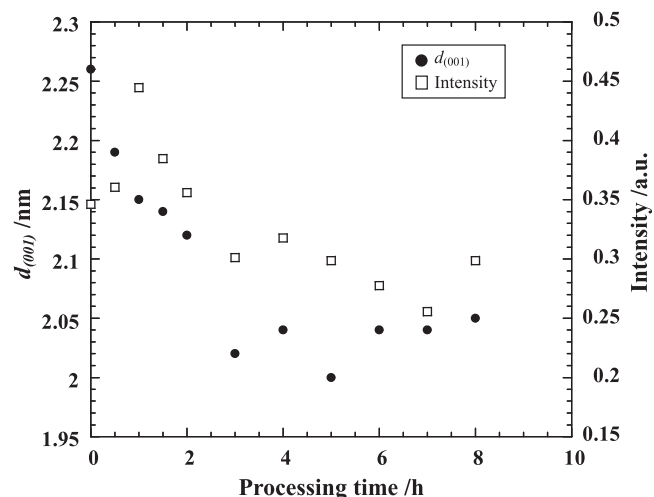


Fig. 2. Time variation of $d_{(001)}$ and corresponding intensity during processing. Intensity is normalized by $\alpha(110)/\gamma(111)$ peak.

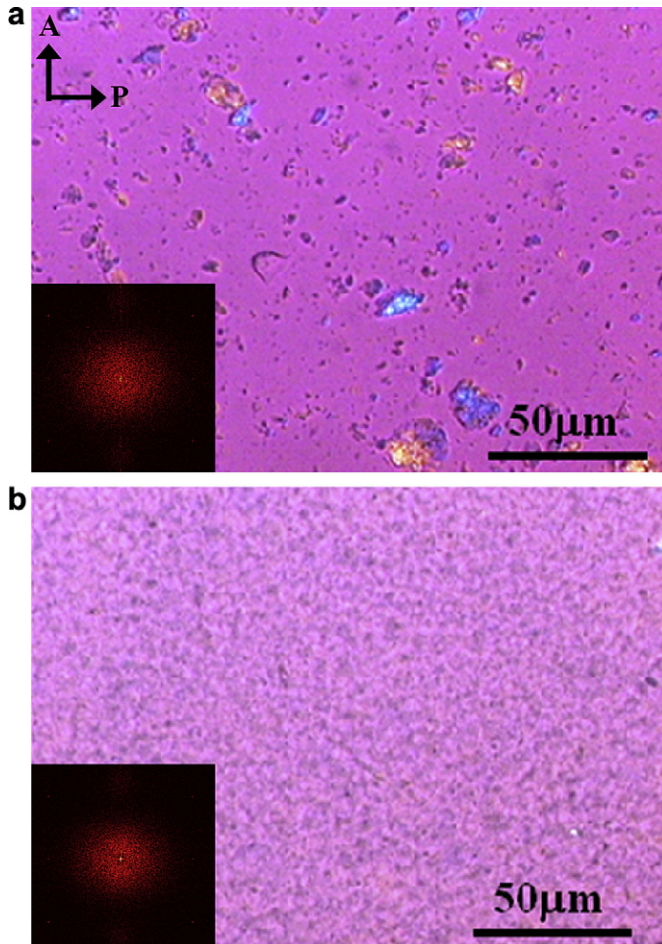


Fig. 3. POM photographs of the mixture (a) unprocessed sample and (b) after solid-state processing for 8 h. Both micrographs were taken at 180 °C just after annealing for 30 s. The inset in each image is a computed FFT spectrum of the micrograph.

for 3 min [17]. The ejected samples were dried under vacuum at 80 °C for 6 h to remove water. The dried nano-composite was then converted into sheets with a thickness of 0.7–2 mm by pressing with ≈ 1.5 MPa at 180 °C for 1 min using a laboratory hot-press (Mini Test Press-10, Toyo Seiki Seisaku-sho, Ltd.). Furthermore, instead of using alumina mortar, we carried out solid-state processing using internal mixer (Laboplastomill V4C150, Toyo Seiki Seisaku-sho, Ltd.) with a rotating speed of 50 rpm at 50 °C for 5 h.

3. Results and discussion

3.1. Variation of WAXD profiles

WAXD patterns for the mixture powder of PP and OMLF (95:5 wt./wt.) are presented in Fig. 1(a). The mean interlayer spacing of the (001) plane ($d_{(001)}$) for the MMT that was modified by C₁₆TBP [MMT-C₁₆TBP] obtained by WAXD measurements is 2.26 nm (diffraction angle, $2\Theta = 3.90^\circ$). Actually, there is a large anisotropy of the stacked silicate layers. The size of the some of the stacked silicate layers appears to reach about 50–100 nm in lengths and the interlayer distance as revealed by TEM observation is about 3 nm (see Fig. 4(a and c)). This value is virtually same as compared to WAXD data.

After solid-state processing for 2 h, a small remnant shoulder is observed around $2\Theta \approx 4.00^\circ$ (Fig. 1(c)). In the following processing from 3 to 8 h, the peak was almost featureless diffraction, only

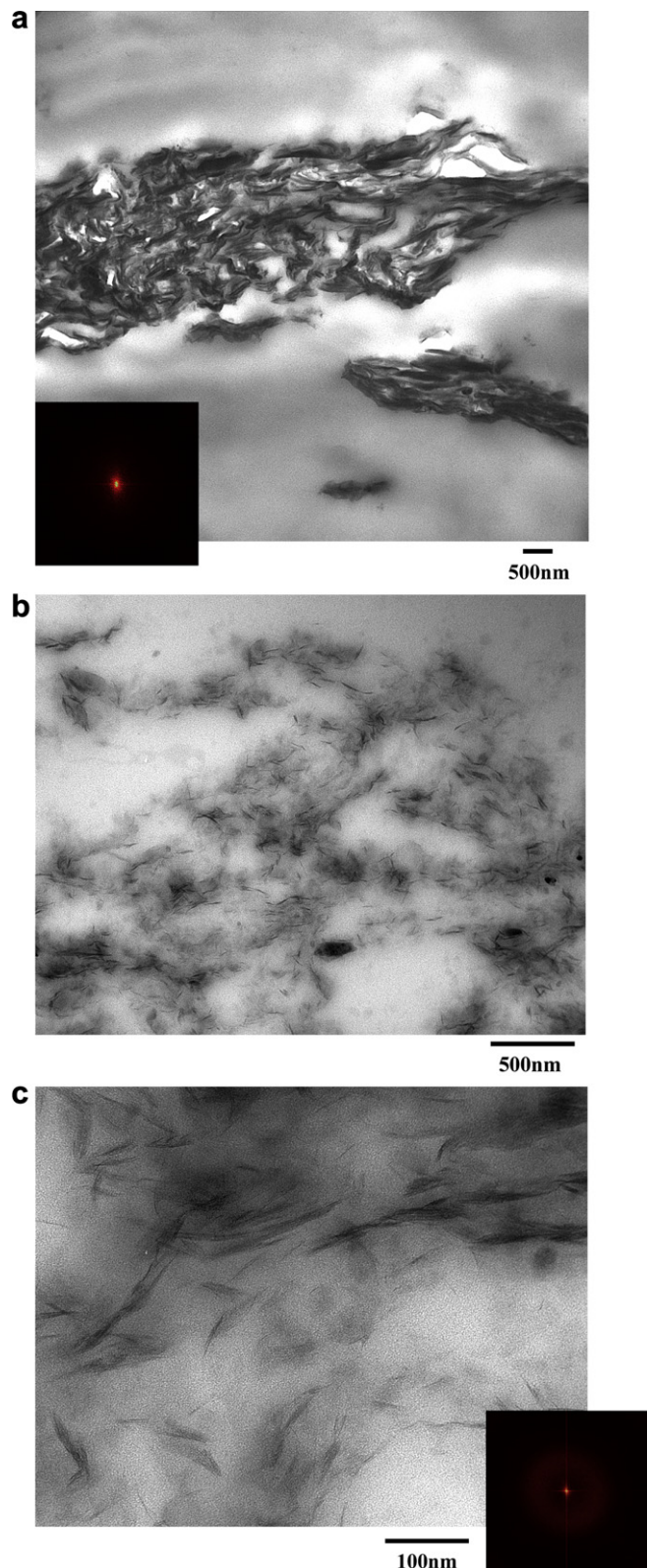


Fig. 4. Bright field TEM images of (a) unprocessed sample, (b) and (c) sample prepared by solid-state processing for 8 h. The dark entities are the cross section and/or face of intercalated-and-stacked silicate layers, and the bright areas are the matrix. The inset in (a) and (c) are a computed FFT spectrum of the micrograph.

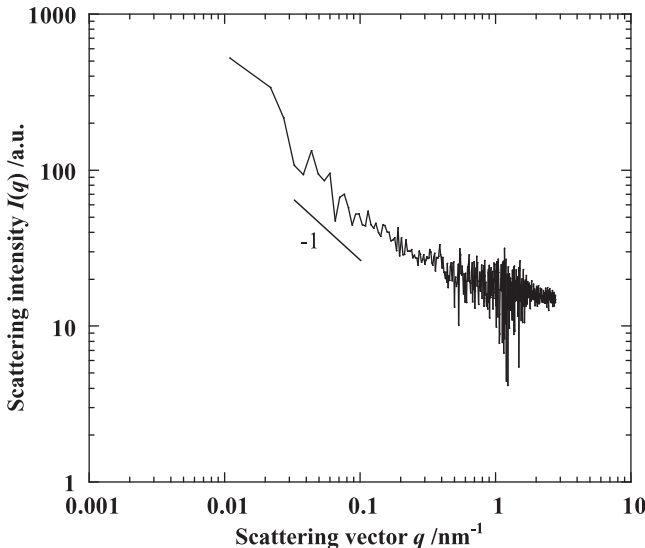


Fig. 5. One-dimensional scattering pattern of processed PP/OMLF for 8 h obtained from FFT analysis. The solid line was drawn by the power law of $I(q) \approx q^{-1}$ at the q range of 0.02–0.2 nm $^{-1}$.

exhibiting the monoclinic (α -form)/triclinic (γ -form) unit cells of the crystallized PP [18].

Fig. 2 shows the time variation of $d_{(001)}$ and corresponding intensity during processing. With increasing processing time the intensity from $d_{(001)}$ gradually decreases with peak shift to lower angle (layer shrinkage). Beyond 4 h, the layer spacing finally reached a constant value (~ 2.05 nm) possibly due to the change of the interdigitated layer structure of the MMT-C₁₆TBP [19]. The structure may suggest that the different orientation angle could adopt, giving a decreasing of the basal spacing during processing.

3.2. Morphology

To elucidate the morphologies before and after solid-state processing, we conducted POM observation at 180 °C Fig. 3(a) shows the POM photograph of the mixtures prepared by melt compounding and annealing at 180 °C for 30 s. It is clear from the POM

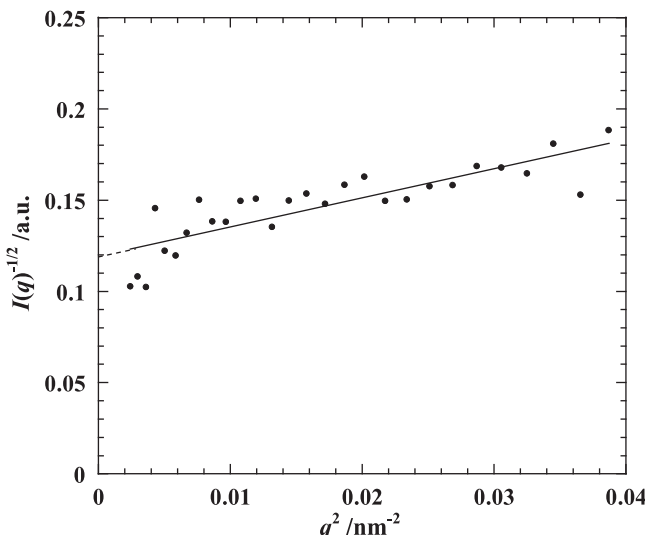


Fig. 6. Debye–Bueche plot for FFT analysis. The solid line is calculated by linear regression. The dashed line indicates the intercept of the plot.

Table 1

Form factors of two nano-composites obtained from TEM and FFT analyses.

Parameters	TEM image	FFT with DB theory
L_{MMT}/nm	67 ± 6	—
t_{MMT}/nm	5.8 ± 0.5	3.7
$\xi_{\text{MMT}}/\text{nm}$	45 ± 2	157

photographs that stacked-and-agglomerated structure of layers is evident in the melt compounded sample, whereas a good dispersion appears in the processed sample for 8 h (Fig. 3(b)). The FFT pattern shows weak scattering with isotropy (halo) as compared with that of unprocessed sample (i.e., melt compounded sample). This indicates that the particles size of the dispersed nano-filler becomes smaller during solid-state processing. The dispersion state in the nanometer scale was directly observed via TEM analysis.

Fig. 4 shows the results of TEM bright field images and their FFT patterns of the melt compounded mixtures corresponding to the POM experiments, in which dark entities are the cross section of the layered nano-fillers. The large agglomerated tactoids of about 3 μm thickness are seen in Fig. 4(a) (unprocessed sample). On the other hand, in Fig. 4(b), nanometer sized thickness layers were straggled in the observation area. Fig. 4(c) shows disorder and delaminated silicate layer structure with the thickness of 3–7 nm and length of 50–200 nm (average thickness of 5.8 nm and length of 67 nm). This is a very interesting observation of the discrete silicate layers.

Fig. 5 shows the one-dimensional scattering pattern obtained from FFT analysis. Here, the scattering intensity ($I(q)$) is shown as a function of the magnitude of the scattering vector (q). We found a broad shoulder around $q \sim 0.02 \text{ nm}^{-1}$ and small remnant peaks in the q range from 0.04 to 0.09 nm^{-1} . The broadness is due to the fact that the dispersed OMLF particles are rather disordered and short-range ordered. The decay of intensity in the q range from 0.02 to 0.1 nm^{-1} can be expected by a power law in the form $I(q) \approx q^{-1}$, suggesting the form factor is the randomly oriented rod. Apparently, this is consistent with the shape of the dispersed OMLF particles in the TEM image (Fig. 4(c)).

We estimated the form factors obtained from TEM images and FFT analysis combined with Debye–Bueche (DB) theory, i.e., average value of the particle length (L_{MMT}), thickness (t_{MMT}), of the dispersed particles and the correlation length (ξ_{MMT}) between the particles. The details of the evaluation were described in our previous paper [20]. The Debye–Bueche equation [21] is applicable in isotropic dense system [22]. The detail procedure for the Debye–Bueche plots was described in our previous paper [23]. To estimate the value of ξ_{MMT} , we employed the Debye–Bueche equation:

$$I(q)^{1/2} = \frac{(8\pi\langle\rho^2\rangle\xi^3)^{1/2}}{(1 + \xi^2 q^2)} \quad (1)$$

where ξ is the long-range structure correlation distance, q is the magnitude of scattering vector, $I(q)$ is the intensity of the scattered light at q and $\langle\rho^2\rangle$ is the mean-square fluctuation of the refractive index. [24].

Fig. 6 shows the Debye–Bueche plot for FFT analysis. The plot is observed to be linear. From the slope and the intercept, we can estimate ξ ($=\text{slope}/\text{intercept})^{1/2}$. Once the value of ξ ($=3.65 \text{ nm}$) is given, other morphological parameters are obtained by

$$\xi_{\text{MMT}} = \frac{\xi}{\phi_{\text{MMT}}} \quad (2)$$

$$t_{\text{MMT}} = \frac{\xi}{(1 - \phi_{\text{MMT}})} \quad (3)$$

where ϕ_{MMT} is the volume fraction of the dispersed phase (MMT particles). The details of the evaluation were described in our previous paper [23]. The results are presented in Table 1.

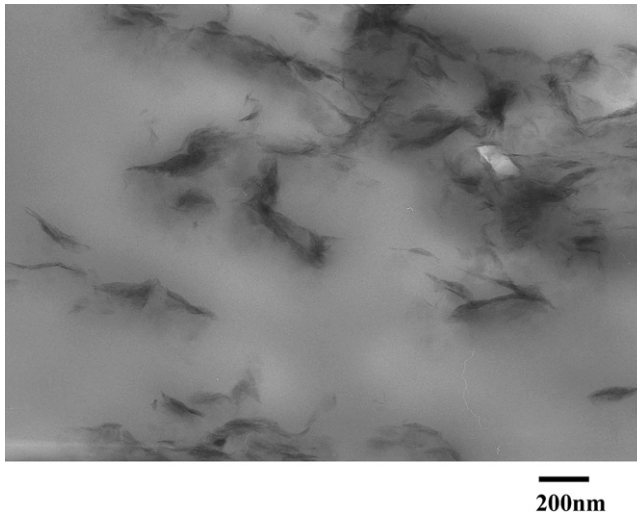


Fig. 7. Bright field TEM image of PP/OMLF (95:5 wt./wt.) prepared by internal mixer with a rotating speed of 50 rpm at 50 °C for 5 h. The dark entities are the cross section and/or face of intercalated-and-stacked silicate layers, and the bright areas are the matrix.

For the sample prepared by annealing without solid-state processing, L_{MMT} and t_{MMT} are in the range of (6–10) μm and (1–3) μm , respectively, as revealed by TEM image (Fig. 4(a)). On the other hand, PP/OMLF prepared by solid-state processing exhibits a small value of L_{MMT} (67 ± 6 nm) with almost double of stacking of the silicate layers ($t_{MMT} = 5.8 \pm 0.5$ nm). ξ_{MMT} value of PP/OMLF with processing (45 ± 2 nm) suggests that a more uniform dispersion of the silicate layers seems to be attained due to the solid-state processing. The absolute value of ξ_{MMT} shows much lower as compared with that of Debye–Bueche plot. The reason is not obvious at present. However, the value of t_{MMT} is virtually same as compared with that of Debye–Bueche plot. After solid-state processing, a stacked silicate layers contain two discrete silicate layers with finer dispersion. This is a unique observation of the discrete silicate layers. The intercalants into nano-galleries act as a lubricant at processing temperature. Since the melting temperature of the intercalant ($C_{16}\text{TBP}^+$) into the nano-galleries was -23.5 °C, we can observe the effect of layer delamination at 65 °C.

Furthermore, we conducted solid-state processing by using internal mixer instead of alumina mortar. For processing with a rotating speed of 50 rpm at 50 °C for 5 h, the dispersed morphology of the silicate layers exhibits same trend with applying pressure (corresponding to the shear stress of 34 MPa) (see Fig. 7). The disordered and delaminated silicate layer structure is observed in TEM image. L_{MMT} and t_{MMT} are in the range of (372 ± 38) nm and (33.2 ± 3.8) nm, respectively. From these facts, the solid-state processing is extremely effective method to collapse the stacked structure in overcoming the pressure drop ($\Delta p \sim 24$ MPa [10]) within the nano-galleries.

To understand the kinetics of the solid-state processing, we attempt to apply a phenomenological formulation for the breakup of mineral particles (Rittinger's law):

$$dE = -b \left[\frac{1}{D^n} \right] dD \quad (4)$$

where E is the energy for breakup, D is the mean diameter of particles and the parameter b and n are the breakup coefficients, which depend on processing condition and materials [25]. The mixing torque T is constant throughout the processing so that the input energy E is proportional to residence time t , i.e., $E \propto T \cdot t$. Hence, eq. (4) can be rewritten as

$$T \cdot t \sim \frac{1}{D^{n-1}} \quad (5)$$

The effect of the different applying torque and residence time on the delamination behavior of the OMLF will be clarified shortly [26].

4. Conclusions

We have described a novel and feasible method for the nano-scale control of the dispersed layered fillers via solid-state processing by using common experimental tools. This processing led to delaminate of the silicate layers and attained the discrete dispersion. This approach can be extended to prepare polymeric nano-composites with delamination of the nano-filters in overcoming the pressure drop within the nano-galleries.

References

- [1] Sinha Ray S, Okamoto M. Prog Polym Sci 2003;28:1539.
- [2] Gardolinski JEFC, Lagaly G. Clay Miner 2005;40:547.
- [3] Usuki A, Kawasumi M, Kojima Y, Okada A, Kurauchi T, Kamigaito O. J Mater Res 1993;8:1179.
- [4] Katoh Y, Okamoto M. Polymer 2009;50:4718.
- [5] Yang K, Ozisik R. Polymer 2006;47:2849.
- [6] Bellair RJ, Manitiu M, Gulari E, Kannan RM. J Polym Sci Polym Phys 2010;48:823.
- [7] Lee EC, Mielewski DF, Baird RJ. Polym Eng Sci 2004;44:1773.
- [8] Zhao L, Li J, Guo S, Du Q. Polymer 2006;47:2460.
- [9] Saito T, Okamoto M, Hiroi R, Yamamoto M, Shiroi T. Macromol Rappid Commun 2006;27:1472.
- [10] Saito T, Okamoto M, Hiroi R, Yamamoto M, Shiroi T. Polymer 2007;48:4143.
- [11] Shao W, Wang Q, Li K. Polym Eng Sci 2005;45:451.
- [12] Shao W, Wang Q, Ma H. Polym Int 2005;54:336.
- [13] Shao W, Wang Q, Wang F, Chen Y. J Polym Sci Polym Phys 2003;44:249.
- [14] Wakabayashi K, Pierre C, Dikin DA, Ruoff RS, Ramanathan T, Brinson IC, et al. Macromolecules 2008;41:1905.
- [15] Masuda J, Torkelson JM. Macromolecules 2008;41:5974.
- [16] Kim YH, Okamoto M, Kotaka T. Macromolecules 2000;33:8114.
- [17] Saito T, Okamoto M, Hiroi R, Yamamoto M, Shiroi T. Macromol Mater Eng 2006;291:1367.
- [18] Meille S, Bruckner S, Porzio W. Macromolecules 1990;23:4114.
- [19] Yoshida O, Okamoto M. Macromol Rapid Commun 2006;27:751.
- [20] Sinha Ray S, Yamada K, Okamoto M, Ogami A, Ueda K. Chem Mater 2003;15:1456.
- [21] Debye P, Bueche AM. J Appl Phys 1949;20:518.
- [22] Hsiao BS, Stein RS, Deutscher K, Winter HH. J Polym Phys 1990;28:1571.
- [23] Okamoto M, Inoue T. Polym Eng Sci 1993;33:175.
- [24] Okamoto M, Inoue T. Polymer 1995;36:2736.
- [25] Bond FC. Mining Eng 1952;4:484.
- [26] Saito T, Okamoto M, in preparation.